Lrg1 inhibits the activation of hepatic macrophages to alleviate NAFLD by enhancing TGF-β1 signaling

LONGFEI XU
Guizhou Medical University
JING HAN
Guizhou Medical University
ZHE YANG
Guizhou Medical University
YANPING YANG
Guizhou Medical University
JINHUI CHEN
Guizhou Medical University
XIJUN WU
Guizhou Medical University
YAN HONG
Guizhou Medical University
Qi Wang (huo2014zhe@163.com)
Guizhou Medical University https://orcid.org/0000-0002-4882-9032

Research Article

Keywords: leucine rich α-2-glycoprotein 1, hepatic macrophages, non-alcoholic fatty liver disease, TGF-β1, steatosic, immune cells

Posted Date: March 28th, 2022

DOI: https://doi.org/10.21203/rs.3.rs-1440311/v1

Abstract

Background: Non-alcoholic fatty liver disease (NAFLD) is caused by excessive hepatic lipid deposition, and is characterized by hepatocyte steatosis, the accumulation of immune cells and the increased expression of inflammatory factors. Hepatic macrophages are the main hepatic immune cells, which play a decisive role in NAFLD. The inhibition of the M1 polarization of hepatic macrophages or the depletion of hepatic macrophages can alleviate hepatic steatosis and inflammation.

Methods and Results: NAFLD mouse model was established by feeding high fat diet (HFD) for 16 weeks, the expression of Lrg1 in liver tissues was detected by Real-time PCR and Western blot. Then expression of Lrg1 in steatotic hepatocytes was detected by Real-time PCR and Western blot. Finally, Western-blot analysis, Real-time PCR, HE staining and immumohistochemical staining were performed to confirm the Lrg1 inhibits the activation of hepatic macrophages to alleviate NAFLD by enhancing TGF-β1 signaling. The results of present study demonstrated that Lrg1 inhibited the polarization of M1 liver macrophages induced by steatotic hepatocyte-derived conditioned medium by enhancing TGF-β1 signaling, and Lrg1 also alleviated liver inflammation induced by a high-fat diet (HFD) via TGF-β1 signaling. In addition, the expression level of Lrg1 was significantly decreased in liver tissues from mice with HFD-induced steatosis.

Conclusion: Our findings identify that HFD-induced hepatic expression of Lrg1 was significantly downregulated Lrg1 inhibits the infiltration of hepatic macrophages to alleviates fatty liver inflammation through enhancing TGF-β1 signaling.

Introduction

Non-alcoholic fatty liver disease (NAFLD), caused by excessive lipid deposition in the liver due to excessive nutrition, is characterized by hepatocyte steatosis, the infiltration of various inflammatory cells, the activation of hepatic stellate cells and the capillarization of hepatic sinusoid endothelium. NAFLD has become the most common chronic liver diseases in high-income countries (1–3), and is often associated with obesity, insulin resistance and/or type 2 diabetes and other metabolic abnormalities induced by metabolic syndrome (4, 5). Although mild liver steatosis is usually self-limited, NAFLD can progress to cirrhosis and end-stage liver disease. More importantly, patients with metabolic syndrome and non-alcoholic steatohepatitis (NASH) can also develop hepatocellular carcinoma without undergoing the stage of liver cirrhosis (6, 7). Currently, the treatment of NAFLD mainly relies on lifestyle interventions, such as dietary changes and increased exercise. There is significant uncertainty regarding the drugs (vitamin E, pioglitazone and pentoxifylline) that are used for the treatment of NAFLD (8). Therefore, further understanding of the mechanisms responsible for NAFLD, and in particular, illustrating the cellular and molecular mechanisms that promote the evolution from steatosis into NASH and even cirrhosis or liver cancer, is critical for the development of novel therapeutic approaches.

A large number of researchers have aimed to explore the role of macrophages in NAFLD. In a previous study, through the clinicopathological analysis of biopsies from patients with NAFLD, large $CD68^+$ Kupffer aggregates were found in the liver (9); these tend to be distributed among damaged hepatocytes (10). The aggregation of intrahepatic macrophages occurs in the early stages of NAFLD, and the degree of macrophage aggregation can also play a certain predictive role in the progression of NAFLD (11). As previously demonstrated, in a model of NASH induced by a lipotoxic high-fat diet (HFD) and high-cholesterol diet, a large number of activated macrophages also accumulated in the liver and the pro-inflammatory factors derived from these cells further aggravated NAFLD (12–17). The prerequisites for macrophages to play pro-inflammatory and pro-injury roles in NAFLD include their aggregation and activation in the liver. However, the mechanisms leading to their aggregation and activation in the liver have not yet been clarified, which is the starting point of the present study.

As a member of a highly conserved leucine-rich repeat protein family, leucine rich α-2-glycoprotein 1 (Lrg1) has been shown to be involved in the regulation of a variety of pathophysiological processes, including angiogenesis (18), oncogenesis (19), arthritis (20) and skin repair (21). In these previous studies, the effect of Lrg1 on specific cell proliferation and migration was often focused on; however, little attention was paid to the effect of Lrg1 on the establishment of the immune microenvironment during these pathological processes. In particular, considering that the processes of angiogenesis (22), tumorigenesis (23) and tissue repair (24) are often accompanied by the transformation of immune cell phenotypes, it was hypothesized that the altered expression of Lrg1 may also affect the immune microenvironment. Since Lrg1 is mainly produced by the liver, the intrahepatic tissue microenvironment may be directly affected by the change in Lrg1 expression.

In the present study, on the basis of finding that the expression of Lrg1 was significantly decreased in fatty liver tissues and steatotic hepatocytes, it was hypothesized that the inhibition of Lrg1 expression induced by steatosis may be a main factor affecting the activation of intrahepatic macrophages. Through *in vivo* and *in vitro* validation assays, a previously neglected immunoregulatory function of Lrg1 was identified, in which Lrg1 appeared to inhibit the M1 polarization of hepatic macrophages by enhancing TGF-β signaling.

Materials And Methods

Establishment and experimental grouping of mouse models of NAFLD. 6-8-week-old female or male BALB/c mice (20 ± 4 g) were purchased from SPF (Beijing) Biotechnology Co., Ltd., and raised at the Animal Center of the Laboratory of Guizhou Medical University in an environment with 22 ± 2˚C, 50–60% humidity and 12-h circulating lighting and provided with unrestricted access to chow and tap water throughout the duration of the present study. All animal experiments were approved by the Experimental Animal Ethics Committee of Guizhou Medical University (approval no. 1900035). To induce the development of NAFLD, 6-weeks-old female or male BALB/c mice (18 ± 2 g) were randomly divided into normal diet (n = 6) and HFD (D12492;Roden Diet with 60 kcal% fat, n = 6) fed for 16 weeks. To investigate whether Lrg1 improves HFD-induced NAFLD by enhancing TGF-β signaling, after being fed a HFD for 16

weeks, then the mice were divided into four groups (n = 6/group), the mice were injected with Lrg1 (50 μg/kg; cat. no. 7890-LR; R&D Systems, Inc.), TGF-β1 (500 ng/kg; cat. no. 1218209; PeproTech, Inc.) or TGF-β1 (500 ng/kg) in combined with Lrg1 (50 μg/kg) through the caudal vein three times (once/5 days). For all mouse experiments, the method of euthanasia was cervical dislocation. The serum samples (500 μl) were additionally collected from the angular veins of the mice.

Cell culture and treatment. Primary hepatocytes were cultured with RPMI-1640 medium (Gibco; Thermo Fisher Scientific, Inc.) containing 10% FBS (Gibco; Thermo Fisher Scientific, Inc.), and were used in the experiments at a confluency of 85%. Primary hepatocytes were treated with or without oleic acid (0.5 mmol/l) for 24 h, and then stained with Oil Red O for 15 min at room temperature (cat. no. G1262; Beijing Solarbio Science & Technology Co., Ltd.) to determine the deposition of lipid droplets according to the manufacturer's instructions.

Isolation and culture of primary hepatocytes. The 8-weeks-old female or male BALB/c mice (21 ± 3 g) were anesthetized by intraperitoneal injection of 1% pentobarbital sodium (150 mg/kg), and then sacrificed by cervical dislocation for perfusion with 20 ml D-Hank's buffer (cat. no. H1045; Beijing Solarbio Science & Technology Co., Ltd.) and 15 ml 0.1% collagenase Ⅱ (cat. no. C8160; Beijing Solarbio Science & Technology Co., Ltd.) successively. When the livers acquired a gray color, they were cut up and resuspended with 10 ml RPMI-1640 medium. The cell suspensions were filtered using a 70-μm cell filter mesh and centrifuged at 55 x g for 3 min at 4℃ to collect the cell precipitates, which were rich in hepatocytes (25). After resuspending with RPMI-1640 medium containing 10% FBS, the cells were cultured in culture plates pre-coated with rat tail collagen I type (cat. no. C8062; Beijing Solarbio Science & Technology Co., Ltd.). In order to induce steatosis, primary hepatocytes were treated with 0.5 mmol/l oleic acid for 24 h, and the medium was replaced with fresh medium for a further 12 h. For subsequent experiments, the conditioned medium (CM) was collected through centrifugation at 2,000 x g for 5 min at 4℃.

Isolation and culture of mouse liver macrophages. The 8-weeks-old female or male BALB/c mice (21 ± 3 g) were anesthetized by intraperitoneal injection of 1% pentobarbital sodium (150 mg/kg),The liver perfusion method was similar to the aforementioned description. When the livers acquired a gray color, they were cut up and suspended with 10 ml D-Hank's buffer for centrifugation at 50 x g for 5 min at 4℃. The cell precipitation was collected for suspension with 20 ml 0.05% collagenase IV for 40 min of shaking in a water bath at 37˚C. Following filtration with 70-μm cell filter mesh, the supernatant was centrifuged at 700 x g for 6 min at 4˚C, and the cell precipitates were suspended with 30% Percoll (cat. no. P8370, Beijing Solarbio Science & Technology Co., Ltd.) and > 50% Percoll of the same volume was then added. Following centrifugation for 8 min at 700 x g at 4˚C, the cells at the adjacent interface of 30% Percoll and 50% Percoll were collected and mixed with an equal volume of D-Hank's buffer. The cell suspension was centrifuged for 6 min at 700 x g at 4˚C, and the precipitate was resuspended in RPMI-1640 medium containing 10% FBS (26). Following 20 min of culture in the culture plate, the medium was replaced with fresh medium, and the cells attached to the wall were liver macrophages.

Western blot analysis. The collected primary hepatocytes or liver tissues were lysed with RIPA buffer (P0013B; Beyotime Institute of Biotechnology) containing 1% PSMF, and centrifuged at 12,000 x g at 4˚C in a centrifuge (Thermo Fisher Scientific, Inc.) for 20 min. Protein concentrations were determined using a Bicinchoninic Acid assay kit (P0010; Beyotime Institute of Biotechnology). Following denaturation with sample loading buffer and electrophoresis with 10% SDS-PAGE gel (cat. no. P0690; Beyotime Institute of Biotechnology), the proteins were transferred to PVDF (cat. no. IPVH00010; EMD Millipore) membranes. Following inoculation with 5% skimmed milk powder (cat. no. 7BF0330; Yili Group) at room temperature for 4 h, the membranes were incubated at 4˚C with anti-inducible nitric oxide synthase (iNOS) antibody (1:1,50; cat. no. D6B6S; Cell Signaling Technology, Inc.) or anti-GAPDH antibody (1:2,000; cat. no. D16H11; Cell Signaling Technology, Inc.) for 16 h, and then incubated with HRP-labeled secondary antibodies (1:3,000; cat. no. ANR02-1; NeoBioscience) at room temperature for 2 h. After washing with TBS-Tween 20, the expression of special protein was detected using an ECL reagent (cat. no. WBKLS0500; EMD Millipore) using a chemiluminescence imager (CLINX5600, Clinx Science Instruments Co., Ltd.).

Reverse transcription-quantitative PCR (RT-qPCR). Total RNA was extracted from the collected primary hepatocytes or liver tissues using TRIzol® reagent (cat. no. 252610; Thermo Fisher Scientific, Inc.), and Monscript™ RTIIIAll-in-One Mix with dsDNase (cat. no. MR05101; Monad Biotech Co., Ltd.) was used to synthesise cDNA. The PCR reaction was performed according to the MonAMP™ SYBR-Green Qpcr Mix (cat. no. MQ10101S; Monad Biotech Co., Ltd.) experimental steps. The expression of specific genes was normalized according to the expression of GAPDH. The RT-qPCR conditions were as follows: 95˚C for 30 sec, 40 cycles of amplification (95˚C for 10 sec, 60˚C for 10 sec, and 72˚C for 30 sec). The primer sequences (Beijing Qingke Biotechnology Co., Ltd.) were as follows (27): Lrg1 (human) forward, 5'-CCTCTTGGAGCAGACAGCG-3' and reverse, 5'-CAGGTGGTTGACAGGAGATGGA-3'; Lrg1 (mouse) forward 5'-TCTTGGCAGCATCAAGGAAG-3' and reverse, 5'-TGGACAGTGTCGGCAGGGA-3'; iNOS (mouse) forward, 5'-GAGCGAGTTGTGGATTGTC-3' and reverse, 5'-CCAGGAAGTAGGTGAGGG-3'; chemokine (C-X-C motif) ligand 1 (CXCL-1; mouse) forward, 5'-CCAAACCGAAGTCATAGCC-3' and reverse, 5'-AGGGAGCTTCAGGGTCAA-3'; interleukin (IL)-1β (mouse) forward, 5'-GTTCCCATTAGACAACTGC-3' and reverse, 5'-GATTCTTTCCTTTGAGGC-3'; GAPDH (human) forward, 5'-GGAGTCCACTGGCGTCTT-3' and reverse, 5'-GAGTCCTTCCACGATACCAA-3'; and GAPDH (mouse) forward, 5'-TGTTTCCTCGTCCCGTAG-3' and reverse, 5'-CAATCTCCACTTTGCCACT-3'.

Immunohistochemical analysis. After being fixed with 4% paraformaldehyde solution for 24 h, the liver tissues were successively placed in 70, 80, 95 and 100% alcohol, a mixture of 50% benzene and 50% alcohol and 100% benzene for 1 h each. The liver tissues were embedded in paraffin and then sliced into 5-µm-thick sections. They were kept in xylene for 30 min, followed by 100, 95 and 70% alcohol for 3 min each to dewax the sections, which were then stained with hematoxylin and eosin at room temperature for 5 min each, successively. For detecting the expression of F4/80, the dewaxed sections were blocked with 3% hydrogen peroxide and then sealed with goat serum (cat. no. SL038; Beijing Solarbio Science & Technology Co., Ltd.) for 30 min. The sections were then incubated with F4/80 (1:200; cat. no. ab6640; Abcam) at 4˚C for 14 h, followed by incubation with HRP Polymer (cat. no. ANR02-1; NeoBioscience) at

37˚C for 30 min. The expression of F4/80 was then observed by DAB staining (cat. no. ZLI-9018; Beijing Zhongshan Jinqiao Biotechnology Co.).

Intraperitoneal glucose tolerance test. After the mice were fasted for 16 h, the blood glucose concentrations were measured, and then re-measured at 15, 30, 60 and 120 min following an intraperitoneal injection of glucose (2 mg/g; cat. no. H50021025, Chuanyu, Chong Qing He Ping Pharmaceutical Co.,Ltd.).

Liver function test. Blood collected from the mice was centrifuged at 500 x g for 10 min at room temperature to collect serum. The contents of aminotransaminase, alanine aminotransaminase, total cholesterol (TC) and triglycerides (TG) in serum were detected using an automatic biochemical analyzer (model: XC8001, Sichuan Xincheng Biological Co., Ltd. China).

Statistical analysis. Data were analyzed using GraphPad Prism v5.01 (GraphPad Software, Inc.) and all data are presented as the mean ± SEM of at least three independent experiments. Differences between two groups were analyzed using a unpaired ‘t’-test, and differences among multiple groups were determined by one-way ANOVA followed by the least significant difference test. $P < 0.05$ was considered to indicate a statistically significant difference.

Results

Lrg1 expression is decreased in livers of mice with hepatic steatosis. In order to investigate the changes in the expression of hepatic Lrg1 occurring during the formation of NAFLD, the development of NAFLD was induced by a HFD. As shown in Fig. 1A, after the mice were fed a HFD, there was a large amount of lipid deposited in the liver tissues, the volume of hepatocytes was enlarged and the hepatic sinuses had narrowed. In addition, a greater number of infiltrating $F4/80^+$cells was observed (Fig. 1B). Additionally, the expression levels of iNOS, CXCL-1 and IL-1β were increased in the livers of mice with NAFLD (Fig. 1C), and the expression of hepatic Lrg1 was downregulated due to steatosis (Fig. 1D and E).

Lrg1 xpression is decreased in steatotic hepatocytes. It has been identified that Lrg1 is mainly expressed in the liver (28). The present study thus examined the effect of steatosis on the expression of Lrg1 in hepatocytes. As shown in Fig. 2A, treatment with oleic acid (0.5 mmol/l) for 24 h resulted in the evident deposition of lipid droplets in primary hepatocytes, and the protein and mRNA expression levels of Lrg1 were significantly suppressed due to steatosis (Fig. 2B and C).

Lrg1 inhibits the activation of hepatic macrophages induced by CM derived from steatotic hepatocytes via TGF-β signaling. To explore the effect of Lrg1 on the activation of hepatic macrophages, primary hepatic macrophages were stimulated with CM derived from steatotic hepatocytes for 12 h, and they were then divided into three groups for treatment with Lrg1 (1 μg/ml), TGF-β 1 (10 ng/ml) or TGF-β 1 (10 ng/ml) in combination with Lrg1 (1 μg/ml) for 24 h. As shown in Fig. 3A, the hepatic macrophages cultured under normal conditions exhibited fewer and shorter processes. Following treatment with CM derived from steatotic hepatocytes, the volume of hepatic macrophages became larger, and increased cell

processes were observed. The morphology of the hepatic macrophages treated with or without Lrg1 was similar. Following stimulation with TGF-β1, the number and length of processes were decreased, and Lrg1 enhanced these reactions. The results of western blot analysis and RT-qPCR revealed that the expression levels of iNOS, CXCL-1 and IL-1β were significantly enhanced by CM from steatotic hepatocytes, while the expression levels of iNOS, CXCL-1 and IL-1β were significantly inhibited by TGF-β1; these inhibitory effects were further enhanced by Lrg1 (Fig. 3B and C).

Lrg1 inhibits HFD-induced NAFLD by enhancing TGF-β signaling. Based on the aforementioned observations, the present study further investigated whether Lrg1 can attenuate HFD-induced NAFLD by enhancing TGF-β signaling. After being fed a HFD for 16 weeks, the mice were injected with Lrg1 (50 μg/kg), TGF-β1 (500 ng/kg) or TGF-β1 (500 ng/kg) in combination with Lrg1 (50 μg/kg) through the caudal vein three times (once/5 days). As shown in Fig. 4A and B, the injection of Lrg1 or TGF-β alone slightly reduced the hepatic lipid deposition and decreased intrahepatic macrophage infiltration; however, TGF-β in combination with Lrg1 attenuated hepatic steatosis and liver inflammation induced by HFD to a greater extent. Moreover, TGF-β in combination with Lrg1 significantly improved liver function, inhibited the serum TC and TG content, and improved intraperitoneal glucose tolerance (Fig. 4C-E).

Discussion

Excess lipid deposition is the initiating factor leading to the formation of NAFLD. With the deterioration of hepatocellular functions and damage due to toxic lipids, other intrahepatic cells also undergo a series of biological changes, including the M1 polarization of macrophages, the activation of hepatic stellate cells, the capillarization of hepatic sinusoid endothelial cells, and the aggregation and activation of platelets. The interaction among liver non-parenchymal cells can also further aggravate intrahepatic inflammation, hepatic insulin resistance and abnormal lipid metabolism (29–31). Although the initial cause for the functional changes of these non-parenchymal cells is hepatocyte steatosis, the mechanisms via which the steatosis of hepatocytes affects the normal hepatic microenvironment are not yet fully understood. As the main immune cells in the liver, hepatic macrophages play a crucial role in the construction of the intrahepatic immune microenvironment in NAFLD (32). The present study attempted to clarify the molecular mechanisms of the formation of the intrahepatic immune microenvironment in NAFLD from the perspective of how steatotic hepatocytes affect the activation of hepatic macrophages.

The expression level of Lrg1 in different tissues derived from GDS4164/CfaAffx.29041.1.S1 was selected from the Gene Expression Omnibus database (https://www.ncbi.nlm.nih.gov/geo/). Compared with other organs and tissues, the expression level of Lrg1 is highest in the liver, suggesting that Lrg1 plays an important role in maintaining the normal physiological microenvironment of the liver. Although Lrg1 in the body is mainly synthesized by the liver, it is a secretory glycoprotein that can be transported to different organs via body fluids. When Lrg1 acts on a variety of cells, it plays various biological roles, such as tumor growth and metastasis, the inflammatory response, angiogenesis and tissue repair (21, 33–39). However, even in similar pathological processes, Lrg1 acts on various cells with vastly different biological functions. For example, when acting on glioma (40) and thyroid carcinoma cells (41), it plays a

positive role in promoting the proliferation and migration of cells; however, when acting on squamous cell carcinoma (42) and hepatocellular carcinoma cells (35), it plays an inhibitory role in cell proliferation and migration. However, with regards to Lrg1 and angiogenesis, it also exhibits different functions in the pathological processes of various organs. For example, in the event of heart failure, the inhibition of Lrg1 expression by microRNA-494 has been shown to induce the proliferation and migration of endothelial cells (43). As also previously demonstrated, in a rat model of cerebral ischemia, Lrg1 has been shown to promote angiogenesis by enhancing TGF-β1 signaling (44). In addition, Lrg1 promotes pulmonary fibrosis by enhancing the activation of pulmonary fibroblasts (45), and Lrg1 inhibits the activation of cardiac fibroblasts and improves myocardial fibrosis by suppressing TGF-β1 signaling (46). These studies not only illustrate the significant differences in the effects of Lrg1 on various cells, but also suggest that Lrg1 may function by affecting TGF-β1 signaling.

In several previous studies, it has been clearly demonstrated that TGF-β1 inhibits the transformation of macrophages into a pro-inflammatory phenotype (47–49). In the present study, it was thus hypothesized that Lrg1 may influence the activation of macrophages via TGF-β1 signaling. To confirm this hypothesis, hepatic macrophages were stimulated with Lrg1, and it was found that Lrg1 inhibited the activation of hepatic macrophages induced by the CM of steatotic hepatocytes by enhancing TGF-β1 signaling; Lrg1 also inhibited liver inflammation induced by HFD by enhancing TGF-β1 signaling. Furthermore, marked macrophage aggregation and activation was observed in the livers of mice with NAFLD, and it was found that the expression of Lrg1 was significantly decreased in fatty liver tissue. Therefore, it was hypothesized that the decreased expression of Lrg1 induced by hepatocyte steatosis may be the reason for the activation of intrahepatic macrophages. These results suggest that Lrg1 derived from normal hepatocytes plays an important role in the establishment of the hepatic inhibitory inflammatory response microenvironment by enhancing TGF-β1 signaling.

However, while the data obtained herein have revealed some of the mechanisms underlying the role of Lrg1 in hepatic steatosis, certain issues remain unresolved. First, the physiological intrahepatic microenvironment relies on all cells of the liver; thus, whether Lrg1 can also affect the function of other intrahepatic cells to regulate NAFLD warrants further investigation. Second, the signals that regulate the expression of Lrg1 in steatotic hepatocytes need to be determined. Although it has been reported that microRNA-494 inhibits the expression of Lrg1 in endothelial cells (43), it remains unknown whether steatosis affects microRNA-494-mediated Lrg1 expression in hepatocytes. Third, although Lrg1 can attenuate NAFLD by inhibiting hepatic macrophage activity via enhancing TGF-β1 signaling *in vitro* and *in vivo*, the clinical application of ameliorating NAFLD by pharmacologically enhancing the functional activity of Lrg1 is more desirable. The aforementioned questions will be the direction of future research efforts.

Declarations

Acknowledgements

The authors would like to thank the Research Center for Basic Sciences of Medicine in Guizhou Medical University for providing experimemtal equipments, such as fluorescence microscope (NIKON Ti-u-dsri2; Nikon Corporation).

Authors' contributions

QW and YH conceived and designed the experiments. QW, LX, ZY, YY, XW and JC performed the experiments. QW, LX and JH analyzed the data. YH, QW and LX prepared the manuscript. All authors concur with the submission and subsequent revisions submitted and all authors have read and approved the final manuscript. YH and LX confirm the authenticity of the raw data.

Funding

The present study was financially supported by the following grants: The National Nature Science Foundation of China (grant no. 81860154), National Nature Science Foundation of China (grant no. 81960383), The Fund of Guizhou Province Science and Technology Department [grant no. Qiankezhicheng (2018) 2784], Guizhou Medical University Seedling Cultivation and Innovation Exploration Project [grant no. Qiankehe (2018)5779-24], Doctor Initiation Fund of Guizhou Medical University [grant no. Yuanbohe J (2018)002], Open Project Contract of Key Laboratory of Adult Stem Cell Transformation Research, Chinese Academy of Medical Sciences (Guizhou Medical University) (grant no. 2018YB02), Guizhou Provincial Education Department Youth Science and Technology Talent Growth Project [grant no. Qianjiaohe KY (2021)150], and the Guizhou Provincial Education Department Youth Science and Technology talent Growth Project [grant no. Qianjiaohe KY (2018) 172].

Data availability

The datasets used and/or analyzed during the current study are available from the corresponding author on reasonable request.

Conflicts of interest

The authors declare that they have no conflicts of interest.

Ethical approval

All animal experiments were approved by the Experimental Animal Ethics Committee of Guizhou Medical University (approval no. 1900035)

References

1. Chalasani N, Younossi Z, Lavine JE et al (2012) The diagnosis and management of non-alcoholic fatty liver disease: practice Guideline by the American Association for the Study of Liver Diseases,

American College of Gastroenterology, and the American Gastroenterological Association. Hepatology 55:2005–2023

2. Lonardo A, Bellentani S, Argo CK et al (2015) Epidemiological modifiers of non-alcoholic fatty liver disease: Focus on high-risk groups. Dig Liver Dis 47:997–1006
3. Sberna AL, Bouillet B, Rouland A et al (2018) European Association for the Study of the Liver (EASL), European Association for the Study of Diabetes (EASD) and European Association for the Study of Obesity (EASO) clinical practice recommendations for the management of non-alcoholic fatty liver disease: evaluation of their application in people with Type 2 diabetes. Diabet Med 35:368–375
4. Younossi ZM (2019) Non-alcoholic fatty liver disease - A global public health perspective. J Hepatol 70:531–544
5. Marra F, Svegliati-Baroni G (2018) Lipotoxicity and the gut-liver axis in NASH pathogenesis. J Hepatol 68:280–295
6. Paradis V, Zalinski S, Chelbi E et al (2009) Hepatocellular carcinomas in patients with metabolic syndrome often develop without significant liver fibrosis: a pathological analysis. Hepatology 49:851–859
7. Kanwal F, Kramer JR, Mapakshi S et al (2018) Risk of Hepatocellular Cancer in Patients With Non-Alcoholic Fatty Liver Disease. Gastroenterology 155:1828–1837e1822
8. Rinella ME (2015) Nonalcoholic fatty liver disease: a systematic review. JAMA 313:2263–2273
9. Park JW, Jeong G, Kim SJ, Kim MK, Park SM (2007) Predictors reflecting the pathological severity of non-alcoholic fatty liver disease: comprehensive study of clinical and immunohistochemical findings in younger Asian patients. J Gastroenterol Hepatol 22:491–497
10. Lotowska JM, Sobaniec-Lotowska ME, Lebensztejn DM (2013) The role of Kupffer cells in the morphogenesis of nonalcoholic steatohepatitis - ultrastructural findings. The first report in pediatric patients. Scand J Gastroenterol 48:352–357
11. Gadd VL, Skoien R, Powell EE et al (2014) The portal inflammatory infiltrate and ductular reaction in human nonalcoholic fatty liver disease. Hepatology 59:1393–1405
12. Lanthier N, Molendi-Coste O, Horsmans Y, van Rooijen N, Cani PD, Leclercq IA (2010) Kupffer cell activation is a causal factor for hepatic insulin resistance. Am J Physiol Gastrointest Liver Physiol 298:G107–116
13. Tosello-Trampont AC, Landes SG, Nguyen V, Novobrantseva TI, Hahn YS (2012) Kuppfer cells trigger nonalcoholic steatohepatitis development in diet-induced mouse model through tumor necrosis factor-α production. J Biol Chem 287:40161–40172
14. Stienstra R, Saudale F, Duval C et al (2010) Kupffer cells promote hepatic steatosis via interleukin-1beta-dependent suppression of peroxisome proliferator-activated receptor alpha activity. Hepatology 51:511–522
15. Stienstra R, Mandard S, Patsouris D, Maass C, Kersten S, Müller M (2007) Peroxisome proliferator-activated receptor alpha protects against obesity-induced hepatic inflammation. Endocrinology 148:2753–2763

16. Miura K, Yang L, van Rooijen N, Ohnishi H, Seki E (2012) Hepatic recruitment of macrophages promotes nonalcoholic steatohepatitis through CCR2. Am J Physiol Gastrointest Liver Physiol 302:G1310–1321
17. Rivera CA, Adegboyega P, van Rooijen N, Tagalicud A, Allman M, Wallace M (2007) Toll-like receptor-4 signaling and Kupffer cells play pivotal roles in the pathogenesis of non-alcoholic steatohepatitis. J Hepatol 47:571–579
18. Wang X, Abraham S, McKenzie JAG et al (2013) LRG1 promotes angiogenesis by modulating endothelial TGF-β signalling. Nature 499:306–311
19. Zhou Y, Zhang X, Zhang J, Fang J, Ge Z, Li X (2017) LRG1 promotes proliferation and inhibits apoptosis in colorectal cancer cells via RUNX1 activation. PLoS ONE 12:e0175122
20. Wang Y, Xu J, Zhang X et al (2017) TNF-α-induced LRG1 promotes angiogenesis and mesenchymal stem cell migration in the subchondral bone during osteoarthritis. Cell Death Dis 8:e2715
21. Gao Y, Xie Z, Ho C et al (2020) LRG1 Promotes Keratinocyte Migration and Wound Repair through Regulation of HIF-1α Stability. J Invest Dermatol 140:455–464e458
22. Jetten N, Verbruggen S, Gijbels MJ, Post MJ, De Winther MP, Donners MM (2014) Anti-inflammatory M2, but not pro-inflammatory M1 macrophages promote angiogenesis in vivo. Angiogenesis 17:109–118
23. Wang J, Li D, Cang H, Guo B Crosstalk between cancer and immune cells (2019) Role of tumor-associated macrophages in the tumor microenvironment.Cancer Med8:4709–4721
24. Gu S, Dai H, Zhao X, Gui C, Gui J (2020) AKT3 deficiency in M2 macrophages impairs cutaneous wound healing by disrupting tissue remodeling. Aging 12:6928–6946
25. Wan Z, Zhao L, Lu F et al (2020) Mononuclear phagocyte system blockade improves therapeutic exosome delivery to the myocardium. Theranostics 10:218–230
26. Aparicio-Vergara M, Tencerova M, Morgantini C, Barreby E, Aouadi M (2017) Isolation of Kupffer Cells and Hepatocytes from a Single Mouse Liver. Methods Mol Biol 1639:161–171
27. Livak KJ, Schmittgen TD (2001) Analysis of relative gene expression data using real-time quantitative PCR and the 2(-Delta Delta C(T)) Method. Methods 25:402–408
28. Kharbanda AB, Rai AJ, Cosme Y, Liu K, Dayan PS (2012) Novel serum and urine markers for pediatric appendicitis. Acad Emerg Med 19:56–62
29. Bessone F, Razori MV, Roma MG (2019) Molecular pathways of nonalcoholic fatty liver disease development and progression. Cell Mol Life Sci 76:99–128
30. Malehmir M, Pfister D, Gallage S et al (2019) Platelet GPIbα is a mediator and potential interventional target for NASH and subsequent liver cancer. Nat Med 25:641–655
31. Hammoutene A, Rautou PE (2019) Role of liver sinusoidal endothelial cells in non-alcoholic fatty liver disease. J Hepatol 70:1278–1291
32. Kazankov K, Jørgensen SMD, Thomsen KL et al (2019) The role of macrophages in nonalcoholic fatty liver disease and nonalcoholic steatohepatitis. Nat Rev Gastroenterol Hepatol 16:145–159

33. Serada S, Fujimoto M, Terabe F et al (2012) Serum leucine-rich alpha-2 glycoprotein is a disease activity biomarker in ulcerative colitis. Inflamm Bowel Dis 18:2169–2179
34. Wong CC, Tse AP, Huang YP et al (2014) Lysyl oxidase-like 2 is critical to tumor microenvironment and metastatic niche formation in hepatocellular carcinoma. Hepatology 60:1645–1658
35. Zhang Y, Luo Q, Wang N et al (2015) LRG1 suppresses the migration and invasion of hepatocellular carcinoma cells. Med Oncol 32:146
36. Wu J, Yin H, Zhu J et al (2015) Validation of LRG1 as a potential biomarker for detection of epithelial ovarian cancer by a blinded study. PLoS ONE 10:e0121112
37. Zhong D, Zhao S, He G et al (2015) Stable knockdown of LRG1 by RNA interference inhibits growth and promotes apoptosis of glioblastoma cells in vitro and in vivo. Tumour Biol 36:4271–4278
38. Liu YS, Luo XY, Li QR et al (2012) Shotgun and targeted proteomics reveal that pre-surgery serum levels of LRG1, SAA, and C4BP may refine prognosis of resected squamous cell lung cancer. J Mol Cell Biol 4:344–347
39. Wen SY, Zhang LN, Yang XM et al (2014) LRG1 is an independent prognostic factor for endometrial carcinoma. Tumour Biol 35:7125–7133
40. Zhong D, He G, Zhao S et al (2015) LRG1 modulates invasion and migration of glioma cell lines through TGF-β signaling pathway. Acta Histochem 117:551–558
41. Ban Z, He J, Tang Z, Zhang L, Xu Z (2019) LRG1 enhances the migration of thyroid carcinoma cells through promotion of the epithelial–mesenchymal transition by activating MAPK/p38 signaling. Oncol Rep 41:3270–3280
42. Zhang N, Ren Y, Wang Y et al (2020) LRG1 Suppresses Migration and Invasion of Esophageal Squamous Cell Carcinoma by Modulating Epithelial to Mesenchymal Transition. J Cancer 11:1486–1494
43. Su Q, Lv XW, Sun YH, Ye ZL, Kong BH, Qin ZB (2019) MicroRNA-494 Inhibits the LRG1 Expression to Induce Proliferation and Migration of VECs in Rats following Myocardial Infarction. Mol therapy Nucleic acids 18:110–122
44. Meng H, Song Y, Zhu J et al (2016) LRG1 promotes angiogenesis through upregulating the TGF–β1 pathway in ischemic rat brain. Mol Med Rep 14:5535–5543
45. Honda H, Fujimoto M, Serada S et al (2017) Leucine-rich α-2 glycoprotein promotes lung fibrosis by modulating TGF-β signaling in fibroblasts. Physiol Rep 5(24):e13556
46. Liu C, Lim ST, Teo MHY et al (2019) Collaborative Regulation of LRG1 by TGF-β1 and PPAR-β/δ Modulates Chronic Pressure Overload-Induced Cardiac Fibrosis. Circ Heart Fail 12:e005962
47. Wang Y, Han B, Wang Y et al (2020) Mesenchymal stem cell-secreted extracellular vesicles carrying TGF-β1 up-regulate miR-132 and promote mouse M2 macrophage polarization. J Cell Mol Med 24:12750–12764
48. Luo H, Hao Y, Tang B, Zeng D, Shi Y, Yu P (2012) Mouse forestomach carcinoma cells immunosuppress macrophages through transforming growth factor-β1. Mol Med Rep 5:988–992

49. Cheng G, Gao J, Wang L et al (2020) The TGF-β1/COX-2-dependant pathway serves a key role in the generation of OKC-induced M2-polarized macrophage-like cells and angiogenesis. Oncol Lett 20(4):39

Figures

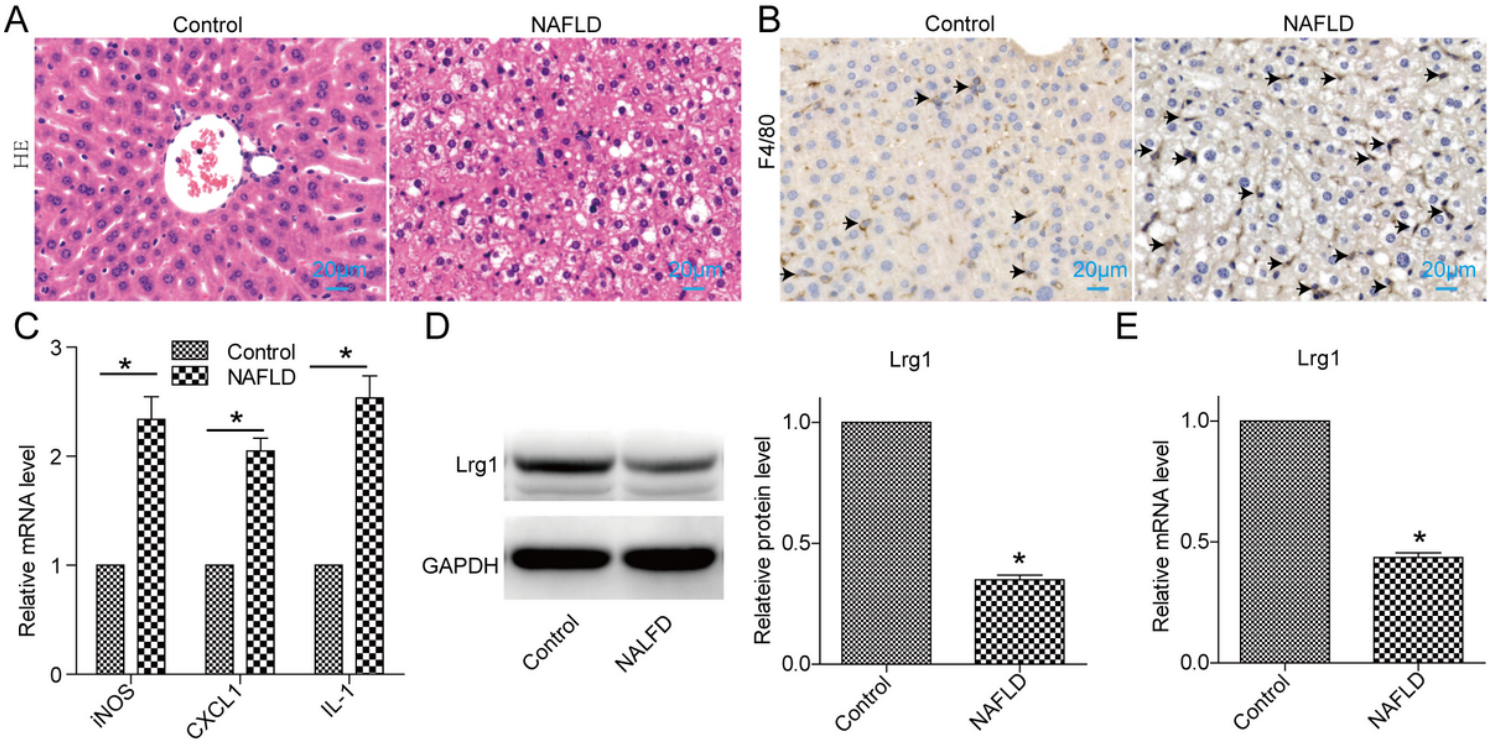

Figure 1

Expression of Lrg1 in normal and steatotic liver tissues. (A) Liver tissues of normal mice and mice with NAFLD were collected for H&E staining. (B) The liver tissues of normal mice and mice with NAFLD were collected to determine the expression of F4/80 by immumohistochemical staining; black arrows indicate $F4/80^+$ cells. (C) Liver tissues of normal mice and mice with NAFLD were collected to detect the expression levels of iNOS, CXCL-1 and IL-1β by RT-qPCR. (D) Expression of Lrg1 in livers from normal mice and mice with NAFLD detected by western blot analysis. (E) Expression of Lrg1 in livers from normal mice and mice with NAFLD detected by RT-qPCR. Scale bar, 20 μm. Data represent the mean ± SEM; n=6 ($^*P<0.05$). Lrg1, leucine rich α-2-glycoprotein 1; NAFLD, non-alcoholic fatty liver disease; iNOS, inducible nitric oxide synthase; CXCL-1, chemokine (C-X-C motif) ligand 1; RT-qPCR, reverse transcription-quantitative PCR.

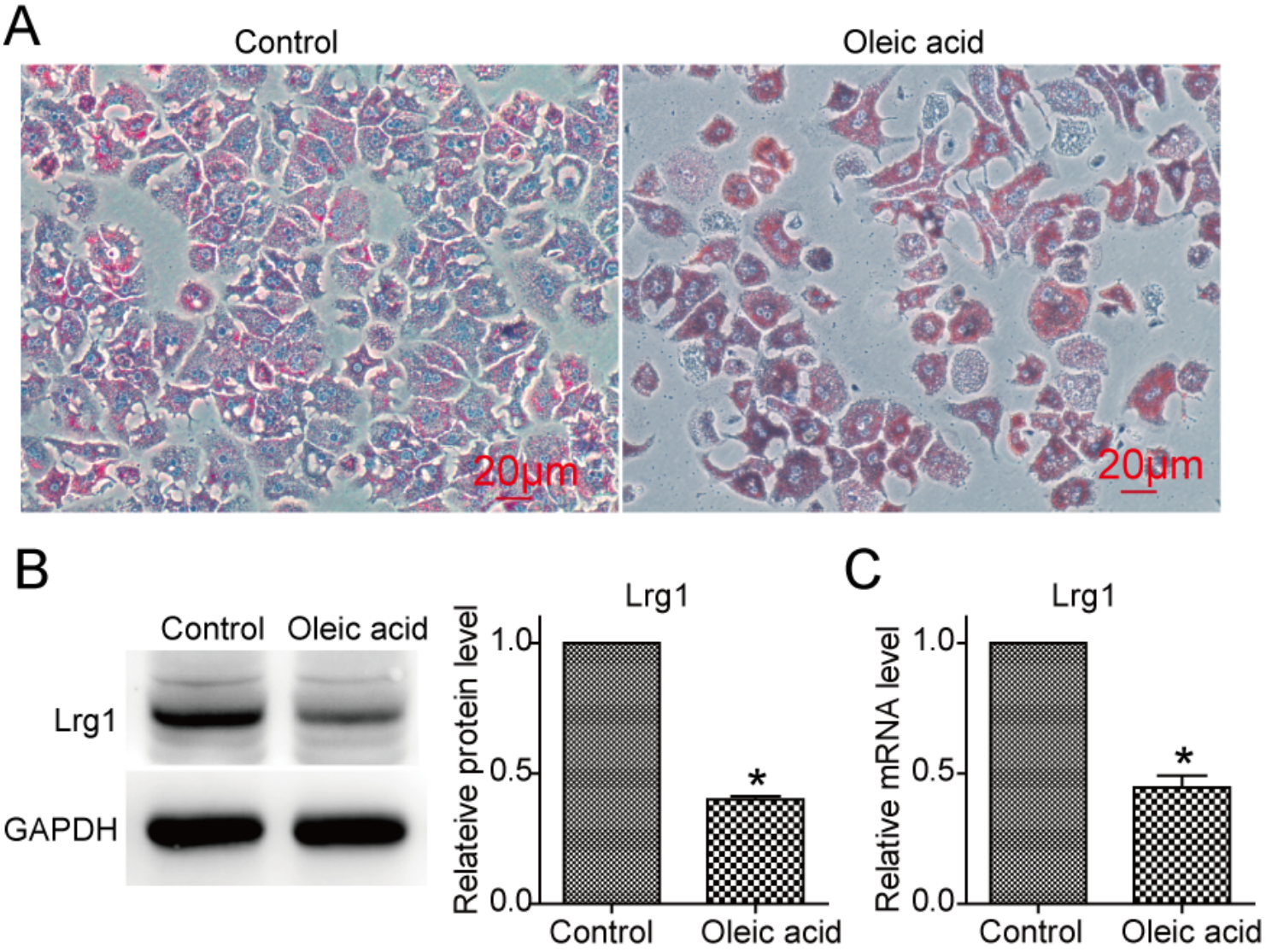

Figure 2

Expression of Lrg1 in normal and steatotic hepatocytes. (A) Primary hepatocytes were treated with or without oleic acid (0.5 mmol/l) for 24 h to determine the deposition of lipid droplets through Oil Red O staining. (B) The expression of Lrg1 was measured by western blot analysis in primary hepatocytes treated with or without oleic acid (0.5 mmol/l) for 24 h. (C) The expression of Lrg1 was measured by RT-qPCR in primary hepatocytes treated with or without oleic acid (0.5 mmol/l) for 24 h. Scale bar, 20 μm. Data represent the mean ± SEM; n=6 ($^{*}P<0.05$). Lrg1, leucine rich α-2-glycoprotein 1; RT-qPCR, reverse transcription-quantitative PCR.

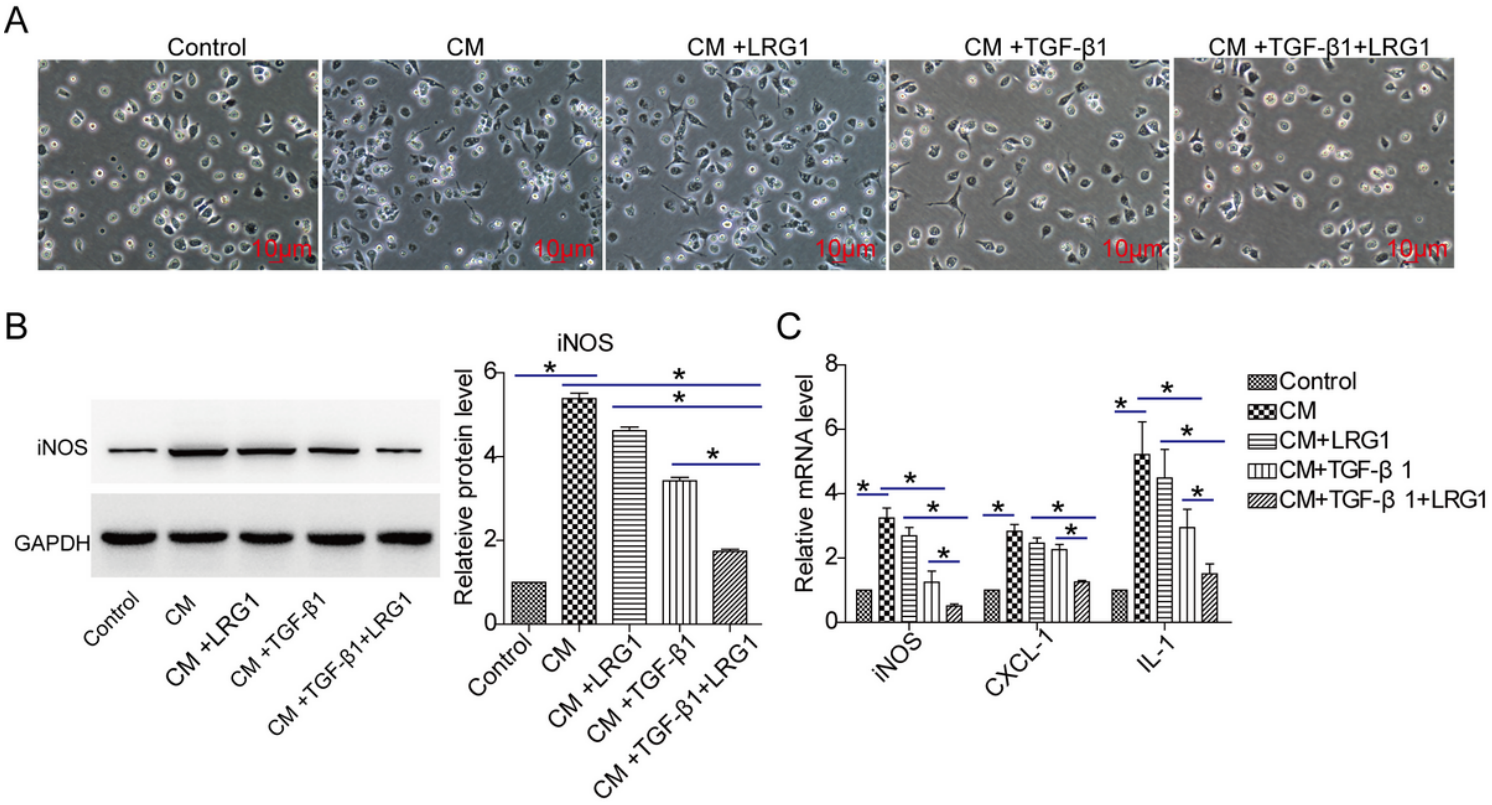

Figure 3

Lrg1 regulates the activation of hepatic macrophages induced by CM derived from steatotic hepatocytes by enhancing TGF-β signaling. Primary hepatic macrophages were stimulated with CM derived from steatotic hepatocytes for 12 h, and were then divided into three groups for treatment with Lrg1 (1 μg/ml), TGF-β1 (10 ng/ml) or TGF-β1 (10 ng/ml) in combination with Lrg1 (1 μg/ml) for 24 h. Normal cultured primary hepatic macrophages were used as controls. (A) Cell morphological changes were observed under an inverted phase contrast microscope. (B) The expression of iNOS was measured by western blot analysis. (C) The mRNA expression of iNOS, CXCL-1 and IL-1β was measured by RT-qPCR . Scale bar, 10 μm. NS, no significance. Data represent the mean ± SEM; n=6 (*P<0.05). Lrg1, leucine rich α-2-glycoprotein 1; CM, conditioned medium; iNOS, inducible nitric oxide synthase; CXCL-1, chemokine (C-X-C motif) ligand 1; RT-qPCR, reverse transcription-quantitative PCR.

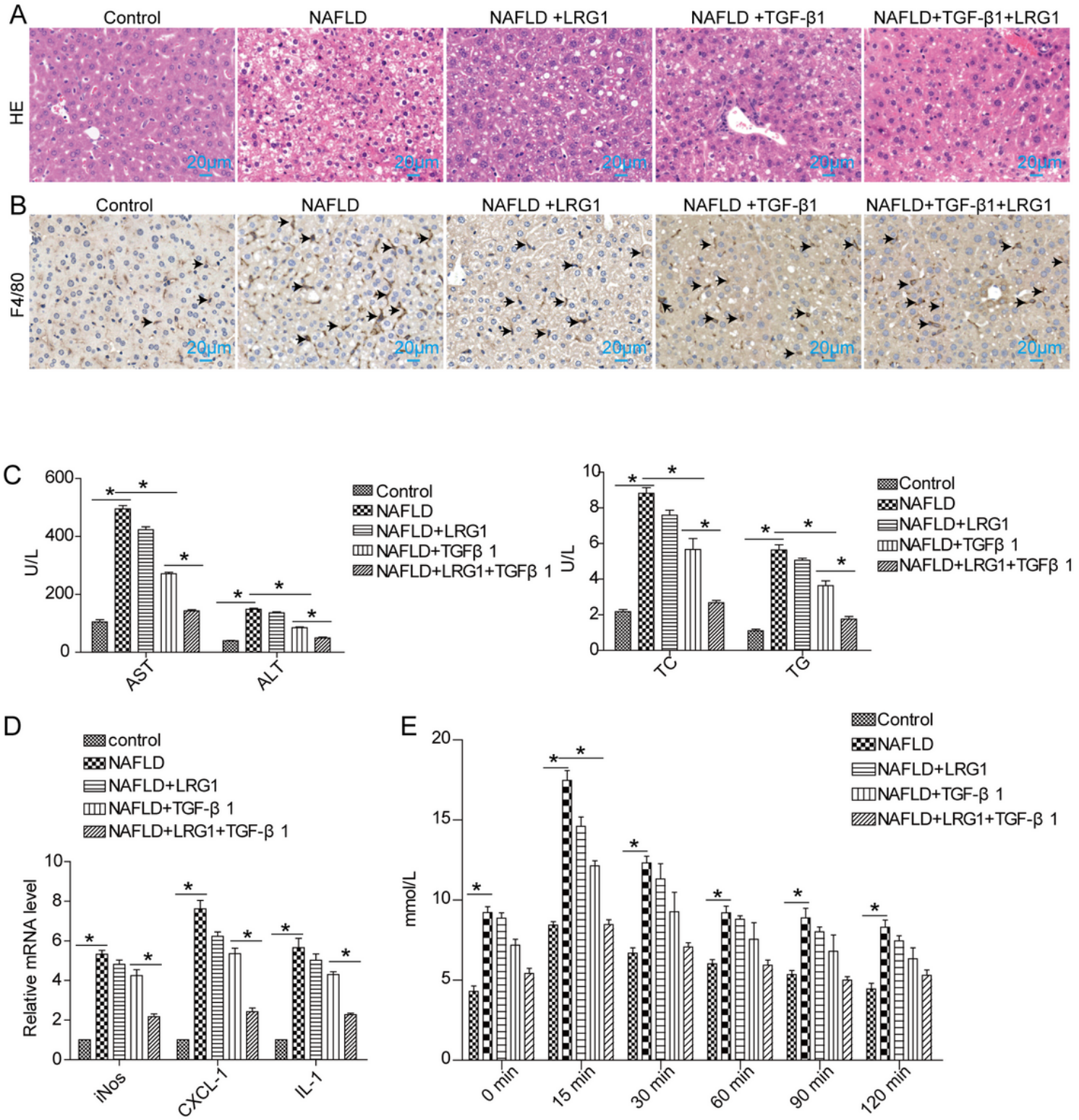

Figure 4

Lrg1 regulates HFD-induced NAFLD by enhancing TGF-β signaling. After being fed a HFD for 16 weeks, mice were injected with Lrg1 (50ug/kg), TGF-β1 (500ng/kg) or TGF-β1 (10 500ng/kg) in combination with Lrg1 (50ug/kg) through the caudal vein three times (once/five days); mice fed a normal diet were used as controls. Liver tissues were collected for (A) H&E staining and (B) for determining the expression of F4/80 through immumohistochemical staining. (C) The contents of AST, ALT, TC and TG in serum were detected

using an automatic biochemical analyzer. (D) The expression levels of iNOS, CXCL-1 and IL-1β in liver tissues were detected by RT-qPCR. (E) Peritoneal glucose tolerance was detected before the serum and liver tissues were collected. Scale bar, 20 μm. NS, no significance. Data represent the mean ± SEM; n=6 ($^{*}P<0.05$). Lrg1, leucine rich α-2-glycoprotein 1; HFD, high-fat diet; NAFLD, non-alcoholic fatty liver disease; AST, aminotransaminase; ALT, alanine aminotransaminase; TC, total cholesterol; TG, triglycerides; iNOS, inducible nitric oxide synthase; CXCL-1, chemokine (C-X-C motif) ligand 1; RT-qPCR, reverse transcription-quantitative PCR.